Sixth International Conference on Durability of Concrete Structures
18 - 20 July 2018
University of Leeds, Leeds, West Yorkshire, LS2 9JT, United Kingdom

Paper Number TIM05

Development of Engineered Cementitious Composites with Conductive Inclusions for Use in Self-sensing Applications

B. Suryanto, D. Saraireh, S. Walls, J. Kim and W.J. McCarter
Heriot-Watt University, Edinburgh, United Kingdom.

ABSTRACT

The mechanical and a.c. electrical properties of a new varietal of engineered cementitious composite (ECC) incorporating conductive inclusions are presented. Electrical measurements were undertaken over a wide frequency range while curing and when under uniaxial tensile loading to study the influence of ongoing hydration and multiple microcrack formation on the composite electrical impedance. When presented in Nyquist format, the work shows that conductive inclusions reduce the bulk resistance of the composite while enhancing its polarizability, transforming the classic, single-arc bulk response of typical cement-based materials to a two-arc response. The bulk resistance was shown to increase with time and damage, the former being due to refinement of pore-structure during hydration. Conductive inclusions smaller than the average microcrack width of ECC were shown to improve the sensitivity of the composite to cracking, while those with high aspect ratio resulted in better electrical continuity at low volume fractions.

Keywords: ECC, damage sensing, hydration, impedance, milled carbon fiber, smart composite.

1.0 INTRODUCTION

Recent decades have seen an increasing interest in the development of structural materials with multi-functional capabilities which demonstrate both structural and non-structural properties. One emerging area of research is the design of self-sensing materials which combine key engineering properties of structural materials with self-monitoring capabilities (McCarter *et al*., 2012; Shi and Chung, 1999; Azhari and Banthia, 2012). With regard to strain-sensing application, work has, in the main, focused on the piezo-resistive response of these materials to mechanical strain.

This work directs attention to use of engineered cementitious composite (ECC) as potential strain-sensing materials. ECC is a family of highly damage-tolerant cement-based composites, known primarily for their superior tensile strain capacity and inherent ability to control crack width. While the ECC itself could be considered as a piezo-resistive material (Saraireh *et al*., 2018), further development is required before it can be made available for use in self-sensing applications.

Figure 1 shows the general concept of the work presented. For use in strain/damage sensing applications, it is desirable to minimise variations in electrical properties due to non-mechanical factors (e.g. cement hydration) to a negligible proportion. The introduction of high aspect ratio conductive material could be beneficial as it offers better electrical continuity at a lower percolation threshold. However, it would be necessary to limit the size of the conductive material to be smaller than, or at least the same order to the average width of micro-cracks in the ECC, in order to maintain, or even improve, the material sensitivity to cracking. To demonstrate this concept, this paper presents the a.c. electrical properties of ECC with and without inclusion of electrically conductive fillers in the mix formulation. Electrical impedance measurements were undertaken over a wide frequency range to identify the frequency range over which the bulk electrical properties provide useful insights with regard to strain/damage sensing.

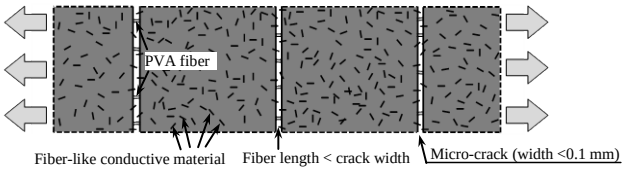

Fig. 1. A schematic showing the proposed concept

2.0 EXPERIMENTAL PROGRAMME

The experimental program involved the testing of three series of ECC specimens, with a total of ten specimens cast for each series: two prisms for electrical testing to study the influence of hydration, five dog-bone specimens for study of the piezo-impedance properties of the material, and three 50 mm cubes for compressive strength testing. Each series was produced with a different material composition.

2.1 Materials

Three different ECC mixes were prepared within this study: a control mix following the normal ECC mix developed by Suryanto *et al.* (2016a); a second mix incorporating conductive sand (CS) as the main aggregate filler; and a third, hybrid mix incorporating both conductive sand and recycled, milled carbon fiber (CS-MC) inclusions. The mix details are presented in Table 1, together with the mean 28-day compressive strength (F_{28}) determined on 50 mm cubes.

Table 1. ECC mix used in the testing programme

Material	Weight per unit volume (kg/m^3)		
	Mix 1	Mix 2	Mix 3
CEM I	454	393	388
Fly-ash	818	707	699
Silica sand	273	–	–
Conductive sand	–	511	505
PVA fibers	26	26	26
MC fibers	–	–	18
HRWR	4.54	4.47	6.67
F_{28} (MPa)	51.8	41.0	47.9

CEM I 52.5N cement to BS EN197-1(2011) and fine fly-ash (Superpozz SV80), at a fly-ash-to-cement (FA/C) ratio of 1.8, were used as the primary binder, with the water/binder ratio kept constant at 0.28 by weight across all mixes. The oxide composition of the FA is presented in Table 2. The aggregate used in the control mix (Mix 1) was fine silica sand with a mean particle size of 120 μm, added at a sand-to-cement ratio of 0.6 by weight. In Mixes 2 and 3, this ratio was increased to 1.3 and the silica sand was replaced by conductive quartz sand (Conductag®, provided by Boud Minerals) with a mean particle size of 275 μm. The quartz sand was supplied with a proprietary conductive carbon resin.

Table 2. Oxide analysis of the fly ash

SiO_2	Al_2O_3	Fe_2O_3	CaO	MgO	Na_2O_{eq}	SO_3	LOI
52.7	26.6	5.6	2.4	1.2	1.7	0.33	<2.0

All three mixes were reinforced with polyvinyl alcohol (PVA) fibers (REC15, Kuraray) at a fixed volume fraction of 2%. The PVA fibers had a mean diameter of 39 μm and length of 12 mm, and a mean tensile strength of 1.6 GPa and tensile strain capacity of 6.5%. The fibers were supplied with a 1.2% (by weight) proprietary oiling agent to reduce excessive bonding with the cement matrix. In addition to the PVA fibers, milled carbon (MC) fibers (supplied by ELG Carbon Fibre) were added in Mix 3 at a dosage of 1% by total volume, to maximize the amount of conductive fillers within the ECC matrix. The MC fibers had an average diameter of 7.5 μm and length of ~100μm. To aid fiber dispersion, a polycarboxylate high-range water-reducing admixture (Master Glenium ACE499) was used at a dosage of, respectively, 1%, 1.15% and 1.7% by weight of cement for Mixes 1, 2 and 3.

2.2 Fabrication and curing

A Hobart planetary motion mixer with 10-litre capacity was used to prepare the specimens. The prisms for electrical testing were cast in polystyrene molds with internal dimensions of 40x40x160 mm (Fig. 2(a)). Prior to casting, two 45×65×2 mm (thick) perforated stainless steel electrodes were placed in the mold at 140 mm spacing. The electrodes had 10 mm diameter holes drilled at 15 mm staggered pitch to allow for infiltration of ECC slurry when being poured into the mold. The dog-bone shaped specimens were cast in Perspex molds with dimensions shown in Fig. 2(b), while the cubes were cast in a standard 3-gang steel mold.

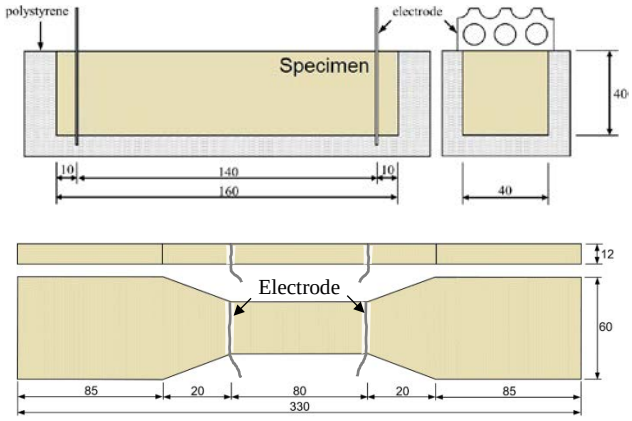

Fig. 2. Dimensions of prismatic specimen for hydration study and dog-bone shaped specimen for piezo-impedance study. All dimensions in mm

After mixing, the ECC slurry was poured in the respective molds and the top surfaces tamped gently to ensure adequate filling. Any excess material was removed and the top surface leveled using a spatula. All specimens were then covered with polyethylene sheeting and placed in a temperature-controlled laboratory (21±1°C, 55±5% RH). The specimens were demolded after 24h and then submerged in water in the same laboratory environment until required for testing.

2.3 Electrical property measurements

A Keysight E4980AL LCR meter was used to perform a logarithmic sweep over the frequency range 20Hz–1MHz at 20 frequency points per decade, with a constant signal voltage of 350 mV. In the hydration study, a Solartron 1260 frequency analyser operating in voltage drive mode at the same signal amplitude was also used to obtain the impedance response of the prismatic specimens over a wider frequency range, viz. 1Hz–10MHz.

Connection to the LCR/frequency analyser was by means of short, individually screened coaxial cables which were connected to the electrodes in the test specimen in two-point mode. During the curing period, wire electrodes were attached at opposing ends of the central neck of the dog-bone specimens for electrical testing. The wires were coated with a metallic silver paint to ensure intimate contact with the specimen surface.

Tensile testing was performed using a 100kN 4206 Instron. Each dog-bone shaped specimen was firstly secured in place at both ends using pneumatic grips and loading was then performed under a displacement rate of 0.5 mm/min. Tensile stresses were determined from load cell readings installed in the Instron, while tensile strains within the central bone-neck region were obtained from the average of two linear variable displacement transducer readings. The two LVDTs were clamped at the opposing ends of the central neck using a pair of plastic mounting blocks. A USB data acquisition system was used to acquire readings from the Instron and LVDTs at a rate of 1 Hz.

In addition to stress and strain readings, sample impedance was continuously monitored on a 3-second continuous loop until failure. For this, the LCR meter was operated at 3 frequency points per decade at 13 spot frequencies over the frequency range 100Hz–1MHz: 100 Hz, 200 Hz, 500 Hz, 1 kHz, 2 kHz, 5 kHz, 10 kHz, 20 kHz, 50 kHz, 100 kHz, 200 kHz, 500 kHz and 1 MHz. This sweep measurement was undertaken automatically using a LabVIEW virtual instrument which was also used to display and acquire impedance data during testing.

3.0 TEST RESULTS AND DISCUSSION

3.1 Impedance Response during Curing

The impedance spectra obtained from the LCR meter at 28- and 91- days curing are presented in Fig. 3(a)–(c) in solid and dashed lines, with frequency increasing from right-to-left (20Hz-1MHz) across the plots. Also presented in the figure are data markers representing the impedance spectra in the frequency range 1Hz–10MHz obtained from identical specimens using the Solartron 1260 impedance analyser at 91-days curing. For reasons of clarity, every second data marker is highlighted.

With reference to Fig. 3(a), it is evident that plain ECC displays a classic impedance response, comprising a semi-circular arc forming the left-hand (high-frequency) side of the plot and a spur forming the right (low-frequency) side resulting from the polarisation at the electrode/specimen interface (McCarter and Brousseau, 1990; McCarter *et al*., 2015). The low-frequency end of the arc and the spur form an intermediate *U-shaped* valley which is typical of a cementitious system containing a small volume of

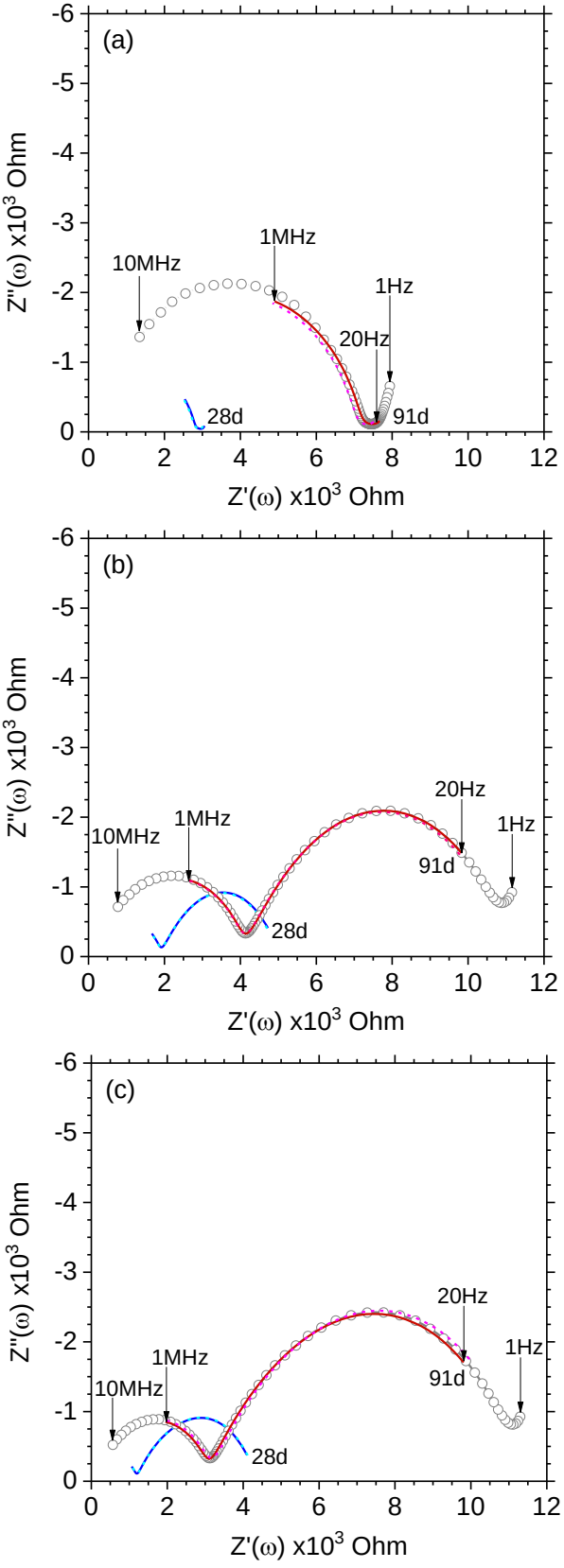

Fig. 3. Impedance response at 28- and 91-day curing: (a) ECC; (b) ECC+CS and (c) ECC+CS+MCF1%.

unburnt carbon from the fly ash (McCarter *et al*., 2004; Suryanto *et al*., 2017a). The intercept of the low frequency end of the arc with the real x-axis gives the bulk resistance. It is apparent from Fig. 3(a) that the bulk resistance increases approximately two-and-a-

half fold from ~2.9kΩ at 28-days to ~7.3kΩ at 91-days curing. This is a direct result of continuous refinement of ECC pore structure resulting from ongoing hydration and pozzolanic reactions.

Figure 3(b) presents the corresponding impedance spectra obtained from ECC+CS specimens containing ~22% conductive sand (carbon powder coated sand) by volume (Mix 2). When compared to the plain ECC, it is evident that the addition of conductive filler transforms the overall impedance response from a *single-* to *double-* bulk-arc response, with the electrode spur still present on the right-hand side of the plot despite being less prominent. It is postulated that the intermediate arc is part of the bulk response and is influenced by induced polarisation at carbon-matrix interface, which is not dissimilar to the interfacial polarisation recently found at the steel-matrix interface within the same composite (Suryanto *et al*., 2016b), while the high-frequency arc represents the bulk composite (Mason *et al*., 2002). Hence the cusp-point between the high-frequency arc and the intermediate arc can be considered as the bulk resistance of the ECC-CS composite (Wansom *et al*., 2006).

With reference to Fig. 3(b), it could be inferred that continuing hydration and pozzolanic reaction still have a notable effect on bulk resistance and overall sample impedance, as indicated by the displacement of the entire spectrum to the right. Regarding the bulk resistance, this was found to increase approximately 2.2 times from ~1.9 kΩ at 28-days to ~4.1 kΩ at 91-days. While the bulk resistance of Mix 2 is lower than that of Mix 1, the increase in bulk resistance indicates that the amount of conductive filler used in this study was still insufficient to eliminate the influence of hydration and pozzolanic activity. This could be attributed to the fact the amount of conductive sand used herein was still below the percolation threshold which, for spherical particles, is in the order of ~30% (Garboczi and Bentz, 1996; Consiglio *et al*., 2003). Thus it could be expected that the conductive sand is still well suspended in the cement matrix and as such, conduction through the composite would be via conductive sand and matrix in series, with the latter being affected by cement hydration.

The impedance response of ECC incorporating conductive sand (CS) at a volume fraction of ~22% and milled carbon fibres (MCF) at a volume fraction of 1% (Mix 3) is presented in Fig. 3(c). Similar overall response and features to those displayed in Fig. 3(b) can be observed, although it is evident from Fig. 3(c) that the addition of milled carbon fibres into the composite results in an increase in the size of the intermediate arc and in a better arc definition, together with a further displacement of the bulk cusp-point to the left. This would imply the contribution of the fibres through conduction via either conductive fillers (CS and MCF) in contact or conductive fillers and matrix in series (McCarter *et al*., 2007). However, cement hydration and pozzolanic reaction still have considerable influence, increasing the bulk resistance ~2.5 times from ~1.2 kΩ at 28-days to ~3.1 kΩ at 91-days.

3.2 Tensile stress-strain response

Figure 4(a)-(c) present representative tensile stress-strain responses from all mixes, together with an example of longitudinal strain profiles during the loading process, obtained using the digital image correlation technique (Suryanto *et al*., 2017b).

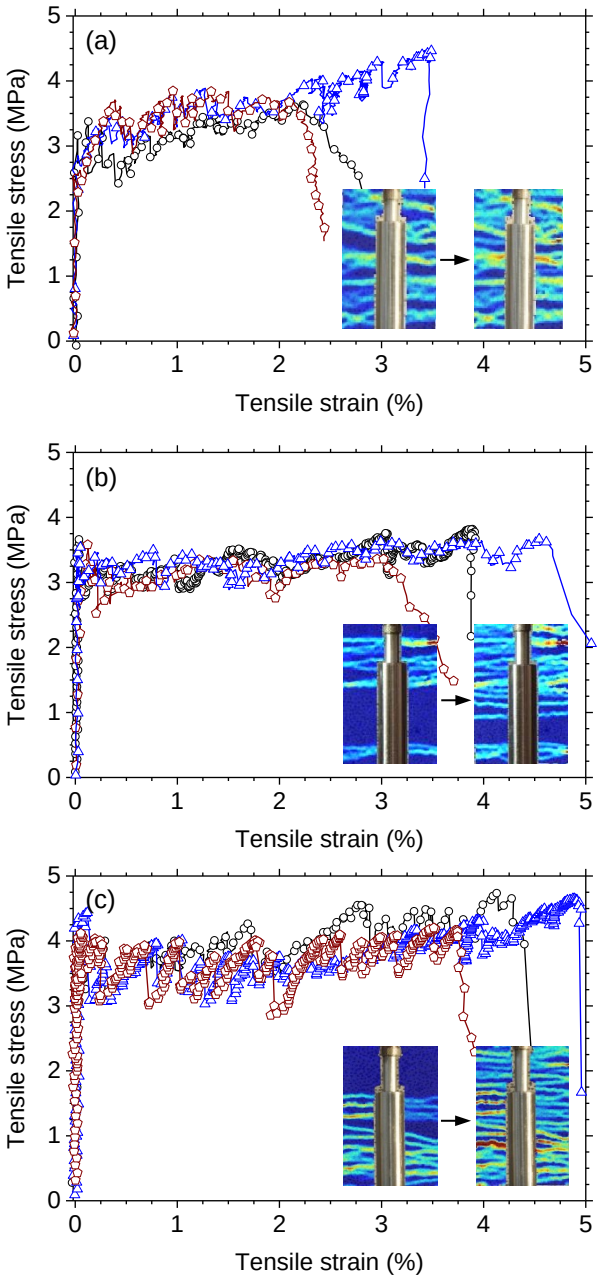

Fig. 4. Tensile stress-strain response: (a) ECC; (b) ECC+CS and (c) ECC+CS+MCF1%.

It is evident from Fig. 4(a) and (b) that the increase in aggregate proportion (~10% to ~22%) and size (100 μm to 275 μm) only slightly altered the post-cracking response of the composite, with a slight reduction in tensile strength apparent in Mix 2. Nevertheless, Mix

2 still displays the unique strain-hardening properties of ECC, achieving a mean tensile strain capacity of ~3.8% and a mean tensile strength of ~3.7MPa and a slight increase in tensile strain capacity. Mix 3 (Fig. 4(c)) displays as good as, if not better, tensile strain-hardening property than the other two mixes.

3.3 Piezo-impedance response

Figure 5(a)–(c) present representative impedance response of the dog-bone specimens produced from, respectively, Mixes 1, 2 and 3 during tensile loading. For reasons of clarity, only the response for every 1% of strain and the one prior failure were plotted. The cusp points and respective strain values are highlighted with an arrow. As before, frequency increases from right to left across the plot.

It is evident from the impedance spectra of Mix 1 displayed in Fig. 5(a) that tensile straining results in a progressive displacement of the plot to the right and an increase in the diameter of the primary arc, resembling the influence of hydration and pozzolanic reaction, as observed earlier in Fig. 3(a). In this instance, however, the increase in sample impedance is as a direct result of the formation and widening of multiple micro-cracks, rather than due to refinement in pore structure from hydration. The bulk resistance increases by ~4.6 times from ~8.5 kΩ at the start of testing to ~39 kΩ just before failure.

With reference to the impedance spectra of Mix 2 (ECC+CS) presented in Fig. 5(b), it is apparent that tensile straining also results in a translation of the spectra to the right albeit at a much smaller magnitude in comparison. Over 4% tensile straining, the bulk resistance increases by a factor of slightly less than two, from ~4.3 kΩ at the start of testing to ~7.5 kΩ just before failure. The slight increase in bulk resistance with increasing strain could be attributed to partial crack bridging by the conductive sand, which is not dissimilar to the influence of crack-bridging conductive fibres reported by Hou and Lynch (2005). Whilst the use of high volume fraction of coarse conductive sand does not significantly alter the strain-hardening properties of the material (see Fig. 4(b)), it reduces the sensitivity of the composite to cracking and, as such, its use in ECC should be explored in other added-function applications.

Fig. 5(c) presents the impedance spectra of Mix 3 (ECC+CS+MCF1%) at various levels of tensile strain (viz, 0–4.3%). It is interesting to note that tensile straining, once again, results in a progressive rightward displacement of the entire spectra. Unlike Mix 2, however, tensile straining also results in an increase in the diameter of the intermediate arc and a progressive upward movement of the cusp point along the y-axis. The increase in the diameter of the intermediate arc would indicate the increasing influence of interfacial polarisation at the carbon-matrix interface with increasing material strain. This could be, in part, attributed to the presence of milledcarbon fibres in which their length is greater than the crack width.

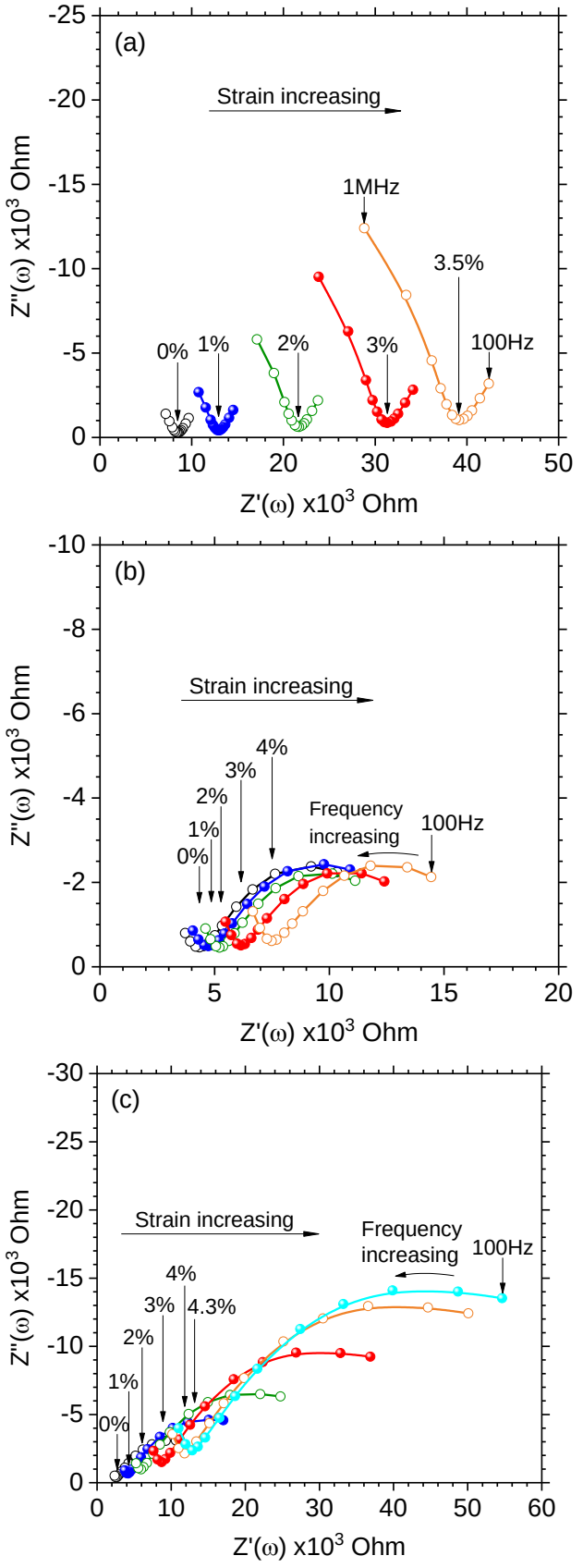

Fig. 5. Piezo-impedance response: (a) ECC; (b) ECC+CS and (c) ECC+CS+MCF1%

As these fibres bridge the micro-cracks, charges develop as current passes across the interface between the cement matrix and the milled carbon fibres, particularly at low frequencies (Suryanto *et al*., 2016b). It is postulated that the apparent increase in the diameter of the intermediate arc with increase in strain is attributed to increasing damage at the milled carbon fibre-matrix interface as the fibres are debonded from the matrix. On application of electrical current, cracked ECC-CS-MCF1% composite will thus have a mixed ionic and electronic conduction process.

Considering the sensitivity to cracking, it is interesting to note from Fig. 5(c) that Mix 3 has a better sensitivity than Mix 2. The bulk resistance is found to increase by a factor of ~4.5, from ~2.6 kΩ at the start to ~11.8 kΩ at the end of testing, which is comparable to the sensitivity of Mix 1.

4.0 CONCLUSIONS

Electrical property measurements were carried out to assess the impedance response of three different ECC mixes while curing and when under tensile loading: plain ECC, ECC containing conductive sand at 22% by volume and ECC with a hybrid mix of conductive sand (22% by volume) and milled carbon fibres (1% by volume). The following conclusions can be drawn from the results presented:

1. It was found that the bulk resistance during the curing period decreases with increasing volume fractions of conductive fillers. The bulk resistance was found to increase by a factor of ~2.5 from 28- to 91-days curing, indicating the influence of cement hydration and pozzolanic activity.

2. When presented in Nyquist format, the addition of conductive fillers was shown to transform the classic, single bulk-arc response to a two-arc bulk response. The emergence of the new arc is due to induced polarisation at carbon-matrix interface.

3. The addition of conductive fillers considered in the present work has been found not to negatively affect the unique strain hardening properties of ECC.

4. Tensile straining was found to displace the entire impedance spectra to the right, indicating an overall increase in impedance with increasing strain. This is as a result of microcrack formation.

5. To maintain, or even improve, the sensitivity of the composite to cracking, the use of conductive inclusions smaller than the average microcrack width of ECC is recommended.

Regarding the potential application of this particular cement composite, the work presented would suggest that the microcrack formation in ECC could be exploited to monitor tension-related damage in a controlled manner.

Acknowledgement

Funding from the Engineering and Physical Sciences Research Council, UK (Research Grants EP/N028597/1) is gratefully acknowledged. The authors also wish to acknowledge material donations from ELG carbon fibre, Boud Minerals, Kuraray GmbH and BASF UK.

References

Azhari, F., Banthia N., 2012. Cement-based sensors for piezoresistive sensing. Cement and Concrete Composites, 34(7):866-873.

BSI, 2011. Cement. Composition, specifications and conformity criteria for common cements. BS EN 197-1:2011.

Consiglio, R., Baker, D.R., Paul, G. , Stanley, H.E., 2003. Continuum percolation thresholds for mixtures of spheres of different sizes. Physica A: Statistical Mechanics & its Applications, 319:49-55.

Garboczi, E.J., Bentz, D.P., 1996. Multi-scale picture of concrete and its transport properties. National Institute of Standards & Technology Internal Report 5900, 52 p.

Hou, T.C., Lynch, J.P., 2005. Conductivity-based strain monitoring and damage characterization of fiber reinforced cementitious structural components. In: Proceedings of SPIE 12th Annual International Symposium on Smart Structures and Materials, San Diego, CA, USA, 2005, pp. 419-430.

Mason, T.O., Campo, M.A., Hixson, A.D., Woo, L.Y., 2002. Impedance spectroscopy of fiber-reinforced cement composites. Cement and Concrete Composites, 24(5): 457-465.

McCarter, W.J., Brousseau, R., 1990. The A.C. response of hardened cement paste. Cement and Concrete Research, 20(6):891-900.

McCarter, W.J., Starrs, G. , Chrisp, T.M., Banfill, P.F.G. , 2007. Activation energy and conduction in carbon fibre reinforced cement matrices. Journal of Materials Science, 42(6):2200-2203.

McCarter, W.J., Starrs, G. , Chrisp, T.M., 2004. The complex impedance response of fly-ash cements revisited. Cement and Concrete Research, 34(10): 1837-1843.

McCarter, W.J., Chrisp, T.M., Starrs, G. , Adamson, A., Owens, E., Basheer, P.A.M., Nanukuttan, S., Srinivasan, S., Holmes, N, 2012. Developments in performance monitoring of concrete exposed to extreme environments. ASCE Journal of Infrastructure Systems, 18(3): 167-175.

McCarter, W.J., Taha, H.M., Suryanto, B., Starrs, G. , 2015. Two-point concrete resistivity measurements : interfacial phenomena at the electrode–concrete contact zone. Measurement Science and Technology, 26(8):085007:1-13.

Shi, Z.Q., Chung, D.D.L., 1999. Carbon fiber-reinforced concrete for traffic monitoring and weighing in motion. Cement and Concrete Research, 29(3):435-439.

Saraireh, B., Walls, S., Suryanto, B., Starrs, G. , McCarter, W.J., 2017. In: Mechtcherine V., Slowik V., Kabele P. (Eds.) Strain-Hardening Cement-Based Composites (SHCC 2017). RILEM Bookseries, 15, Springer, Dordrecht, pp. 292-299.

Suryanto, B., Wilson, S.A., McCarter, W.J., Chrisp, T.M., 2016a. Self-healing performance of engineered cementitious composites under natural environmental exposure. Advances in Cement Research, 28(4):211-220.

Suryanto, B., McCarter, W.J., Starrs, G. , Ludford-Jones, G. V., 2016b. Electrochemical immittance spectroscopy applied to a hybrid PVA/steel fiber engineered cementitious composite. Materials and Design, 105:179-189.

Suryanto, B., McCarter, W.J., Starrs, G. , Chrisp, T.M., 2017a. Characterization of fly-ash using electrochemical impedance spectroscopy. Procedia Engineering, 171:705-714.

Suryanto, B., Tambusay, A., Suprobo, P., 2017b. Crack mapping on shear-critical reinforced concrete beams using an open source digital image correlation software. Civil Engineering Dimension, 19(2):93-98.

Wansom, S., Kidner, N.J., Woo, L.Y., Mason, T.O., 2006. AC-impedance response of multi-walled carbon nanotube/cement composites. Cement and Concrete Composites, 28(6):509-519.